Contribution of mangroves and salt marshes to nature-based mitigation of coastal flood risks in major deltas of the world

Contribution of mangroves and salt marshes to nature-based mitigation of coastal flood risks in major deltas of the world

R. Van Coppenolle[1], C. Schwarz[2], S. Temmerman[1]

[1] Ecosystem Management Research Group, Department of Biology, University of Antwerp, Universiteitsplein 1C, 2610 Wilrijk, Belgium
[2] Coastal Research Group, Department of Physical Geography, Faculty of Geosciences, Utrecht University, P.O. Box 80115, 3508 TC Utrecht, the Netherlands

Corresponding author: Rebecca Van Coppenolle, E-mail: rebecca.vancoppenolle@uantwerpen.be, phone: 0032 3 265 87 12

Abstract

Nature-based solutions are rapidly gaining interest in the face of global change and increasing flood risks. While assessments of flood risk mitigation by coastal ecosystems are mainly restricted to local scales, our study assesses the contribution of salt marshes and mangroves to nature-based storm surge mitigation in 11 large deltas around the world. We present a relatively simple GIS model that, based on globally available input data, provides an estimation of the tidal wetland's capacity of risk mitigation at a regional scale. It shows the high potential of nature-based solutions, as tidal wetlands, to provide storm surge mitigation to more than 80% of the flood-exposed land area for 4 of the 11 deltas and to more than 70% of the flood-exposed population for 3 deltas. The magnitude of the nature-based mitigation, estimated as the length of the storm surge pathway crossing through tidal wetlands, was found to be significantly correlated to the total wetland area within a delta. This highlights the importance of conserving extensive continuous tidal wetlands as a nature-based approach to mitigate flood risks. Our analysis further reveals that deltas with limited historical wetland reclamation and therefore large remaining wetlands, such as the Mississippi, Niger and part of the Ganges-Brahmaputra deltas, benefit from investing in the conservation of their vast wetlands, while deltas with extensive historical wetland reclamation, such as the Yangtze and Rhine deltas, may improve the sustainability of flood protection programs by combining existing hard engineering with new nature-based solutions through restoration of former wetlands.

KEYWORDS: delta, storm surge, mangrove, salt marsh, tidal wetlands, nature-based/ecosystem-based management, risk mitigation

Introduction

Global climate change induces acceleration of sea level rise and is expected to increase the intensity of storm surges, and as such is threatening coastal and deltaic areas worldwide (Hallegatte et al. 2013; Woodruff et al. 2013; Bengtsson et al. 2006; Hinkel et al. 2014). Storm surges originating from severe storms, such as tropical cyclones, propagate from the sea towards the land with surge heights that can reach several meters above mean sea level, causing densely populated low-lying areas in river deltas to be particularly vulnerable to storm surge flood risks (Day et al. 2007; Tessler et al. 2015). Additionally, the globally averaged population density in the Low Elevation Coastal Zone (LECZ, i.e. less than 10 meters above mean sea level) is expected to grow from 241 people/km² in 2015 (i.e. five times the world's average) to 405 to 534 people/km² by 2060 (Neumann et al. 2015; Small and Nicholls 2003; McGranahan et al. 2007).

This increase of both coastal population density and risk probability of coastal flooding events calls for the development of sustainable coastal management strategies. Apart from traditional hard engineered flood defence structures, such as dams or dikes, nature-based or ecosystem-based coastal flood defence is increasingly proposed as an alternative or addition to traditional hard engineering, and relies on the conservation and in certain cases restoration of coastal and deltaic ecosystems (Temmerman et al. 2013; Cheong et al. 2013; Duarte et al. 2013). Here we focus on salt marshes and mangrove forests, which we collectively call tidal wetlands throughout this paper. Among their valuable ecosystem services, tidal wetlands have the capacity to attenuate waves, reduce shoreline erosion and inland storm surge propagation, and to sustain themselves with sea level rise by allochthonous sediment accretion (Gedan et al. 2011; Shepard et al. 2011; Temmerman and Kirwan 2015; Kirwan et al. 2016). As such, nature-based flood risk mitigation is increasingly regarded as a polyvalent, self-adaptive and sustainable strategy (Temmerman et al. 2013).

Observational and hydrodynamic modelling studies have demonstrated the value of tidal wetlands for storm surge mitigation due to the resistance exerted by the wetland vegetation and topography on incoming storm surges, implying a landward attenuation in storm surge height further referred to as storm surge attenuation or reduction (Costanza et al. 2008; Krauss et al. 2009; Wamsley et al. 2010; Zhang et al. 2012; Barbier et al. 2013; Stark et al. 2015). This attenuation is quantified as the rate of vertical reduction in storm surge height per horizontal inland distance over the delta plain (expressed in cm/km). It depends on various factors as the flow resistance provided by the coastal geomorphology and its vegetation or land cover type and on the specific properties of the storm surge, such as its height and duration (Mcivor et al. 2012; Wamsley et al. 2010; Loder et al. 2009; Stark et al. 2015). Observed rates of storm surge attenuation over tidal wetlands range from a couple of cm/km to 25 cm/km (Krauss et al. 2009; Wamsley et al. 2010; Stark et al. 2015), with maximum rates of up to 50 cm/km reported from a hydrodynamic modelling study in Florida's mangroves (Zhang et al. 2012). Although such local to regional observational and modelling studies play an important role in advancing our understanding of the role of tidal wetlands in storm surge risk mitigation, there are no upscaling studies yet that have explored the potential contribution of tidal wetlands to storm surge risk mitigation on a quasi-global scale.

Our study aims to take a first step towards such a global assessment of the contribution of tidal wetlands to nature-based storm surge risk mitigation, by selecting 11 of the most populated deltas around the world. We present results from a GIS model based on globally available data and on relatively simple assumptions to define the storm surge mitigation function of tidal wetlands for low-lying delta areas and populations.

Material and Method

Study areas

For the selection of the studied deltas, the world's deltas were ranked according to their total population size as reported by Ericson et al. (2006). Starting from this list, the selection of the deltas was firstly based on the presence of tidal wetlands, then on the highest population, and lastly on their global distribution, so that at least one delta per continent (North America, South America, Europe, Africa, Asia and Australia) was selected (Table 1).

Some deltas could not be included in the study due to the lack of data regarding the distribution of salt marshes as it is the case for the Pearl River delta in China.

Table 1 Main characteristics and geographical distribution of the deltas selected for the study. A more extensive description of the deltas can be found in the Online Material.

	Country	Tidal wetland type	Population (Ericson et al., 2006)	Delta area as delineated in the study (km²)	Tidal wetlands area within the delta (km²)
Ganges-Brahmaputra delta	India/Bangladesh	Mangrove	111,000,000	78,453.9	6,431.6
Yangtze delta	China	Salt Marsh	42,100,000	61,251.9	121.1
Mekong delta	Vietnam	Mangrove	20,200,000	50,135.2	1,540.4
Chao Phraya delta	Thailand	Mangrove	13,700,000	19,177.3	174.3
Irrawaddy delta	Myanmar	Mangrove	9,720,000	28,744.0	1,252.0
Niger delta	Nigeria	Mangrove	3,730,000	16,714.8	5,646.6
Amazon delta	Brazil	Mangrove	2,930,000	42,028.3	1,676.0
Rhine delta	The Netherlands	Salt Marsh	1,940,000	9,139.9	40.0
Mississippi delta	USA	Salt Marsh	1,790,000	36,894.3	6,014.3
Mahakam delta	Indonesia	Mangrove	706,000	2,425.1	503.5
Burdekin delta	Australia	Mangrove	5,800	1,441.4	129.7

Datasets

The following datasets were used.

The *land elevation* is defined with the NASA Shuttle Radar Topography Mission (SRTM) Global 3 arc second V003 dataset (NASA JPL, 2013). The SRTM dataset is so far the best-known Digital Elevation Model (DEM) available at a global scale (Sun et al. 2003; Rodriguez et al. 2006). It is found to be more accurate in areas with small slopes, such as deltas, yet there can be errors due to reflection of the radar signal on vegetation canopies with an absolute vertical error up to 16 m (http://www2.jpl.nasa.gov/srtm/datafinaldescriptions.html)(Rodriguez et al. 2006; Sun et al. 2003).

The *tidal wetlands distribution* is based on different types of datasets. The representation of mangroves is based on the *Global distribution of mangroves* from the United States Geologic Survey (USGS, www.unep-wcmc.org) (Giri et al. 2011). The distribution of salt marshes is a compilation of different country wide or continent wide datasets as the European Commission program *Corine Land Cover* of 2006 for Europe, the *Geohabitats* for Australia (Heap et al. 2001), the *Classification of Wetlands and Deepwater habitats* for the United States (Federal Geographic Data Committee 2013) and the Chinese wetlands mapping from Niu et al. (2009).

The *storm surge height* is taken from the DIVA database (Hinkel et al. 2014; Vafeidis et al. 2005). It corresponds to the storm surge water level above mean sea level and is calculated by model simulations based on tidal levels, barometric pressures, wind speeds and sea bed slopes for return periods of 10, 100 and 1000 years. The DIVA database uses the coastline of the Digital Chart of the World (DCW, Environmental Systems Research Institute, ESRI, 2002) divided in segments based on administrative and environmental parameters (Vafeidis et al. 2005). To avoid inconsistencies due to differences in scale between the datasets (e.g. tidal wetlands on the seaward side of the DIVA coastline), the DIVA coastline was not directly used as the source of the flooding. Alternatively a 'flood source', i.e. the coastline along the seaward delta front, is interpolated from a convex hull based on the land area (the latter is defined more below). The storm surge heights of the different segments stored in the DIVA coastline are then transferred to the flood source with a shortest Euclidean distance algorithm (for further information see the Online Material).

The *population distribution* originates from the LandScan 2013 Global Population Database (Bright et al. 2013). It represents the population over a 30 arc second grid resolution and integrates the diurnal movements and collective travelling behaviour of the world population, i.e. the so-called "ambient population", averaged over 24 hours (Dobson et al. 2000; Bright et al. 2013). The dataset of 30 arc second resolution was resampled to a resolution of 3 arc second (to match the resolution of the SRTM land elevation dataset) based on the guidelines of the LandScan documentation (Bright et al. 2013; UT BATTELLE LLC.).

The extent of the *world countries* is the representation of the country boundaries as they exist in January 2015 and is available through the ESRI platform (ESRI, DeLorme Publishing Company, Inc., 2015). Due to the fact that the borders of the different global datasets do not perfectly overlap (Lichter et al. 2011), the most seaward extent of the emerging land was defined by merging the extent of the *world countries* dataset and the tidal wetlands datasets, and this land extent is further referred to as the land area.

The *delta areas* were delineated in accordance with spatial delineation of the deltas in other studies (e.g. Syvitski et al. 2009; Coleman et al. 2004).

The global datasets used present some limitations in regards to local data accuracy and local data artefacts. Such limitations may include vegetation artefacts in the SRTM dataset, the moderate resolution of the tidal wetlands datasets, or the static calculation of the storm surge height in the DIVA database.

The resolution of all raster layers was converted to a 3 arc second grid based on the World Geodetic System 1984 ellipsoid, which corresponds to the resolution of the SRTM data grid.

Model description

The model simulates how a storm surge flood wave, entering a delta system from the seaward delta front, would be routed in a landward direction through the channels and over the potential floodplain of the delta, assuming that no artificial flood protecting structures like dikes or dams would be present. It is based on a GIS procedure developed in ArcGIS (10.3.1), and is similar to previously published procedures that assess the coastal areas and number of people vulnerable to storm surge flooding on regional to global scales (Arkema et al. 2013; Dasgupta et al. 2011). The model does not simulate the full complexity of hydrodynamic processes involved in flood propagation and therefore is not able to calculate accurate flood depths and absolute values of reduction in flood depth behind

tidal wetlands. Nevertheless, it has the major advantage to be globally applicable to make a relative comparison between delta systems around the world.

Table 2 Rates of storm surge height attenuation across various tidal wetland types based on observations during storm surges over tidal wetlands areas or on models calibrated by observations

Location	vegetation type	Event	Attenuation rate (cm/km)	Reference
Southern Louisiana	coastal marsh	Compilation of 7 storms between 1909 and 1957	1.6 - 20	United States Army Corps of Engineers (2006)
Louisiana	marsh & open water	Hurricane Andrew (1992), cat. 5	4.4 - 4.9	Lovelace (1994)
Cameron Prairie, Louisiana	marsh	Hurricane Rita (2005), cat. 3	10.0	Wamsley et al. (2010) calculated with data from McGee et al. (2006)
Sabine, Louisiana	Marsh	Hurricane Rita (2005), cat. 3	25.0	Wamsley et al. (2010) calculated with data from McGee et al. (2006)
Vermillion, Louisiana	Marsh	Hurricane Rita (2005), cat. 3	4.0	Wamsley et al. (2010) calculated with data from McGee et al. (2006)
Vermillion, Louisiana	Marsh	Hurricane Rita (2005), cat. 3	7.7	Wamsley et al. (2010) calculated with data from McGee et al. (2006)
Ten Thousand Island National Wildlife Refuge, Florida	mangrove and interior marsh	Hurricane Charley (2004), cat. 3	9.4	Krauss et al. (2009)
Shark River (Everglades National Park) Florida	riverine mangrove	Hurricane Wilma (2005), cat. 3	4.3 - 6.9	Krauss et al. (2009)
Ten Thousand Island National Wildlife Refuge, Florida	mangrove	Hurricane Charley (2004), cat. 3	15.8	Krauss et al. (2009)
Everglades National Park, Florida	Mangrove	Simulations validated with Hurricane Wilma (2005)	20 - 50	Zhang et al. (2012)
Everglades National Park, Florida	no vegetation	Simulations validated with Hurricane Wilma (2005)	6 - 10	Zhang et al. (2012)

The input data of the model is globally available GIS data presented above in combination with the storm surge attenuation rates derived from the range of values found in the literature (Table 2) for the three land cover types considered in this study (Table 3). The open water and channel areas are attributed a very low attenuation value of 0.1 cm/km (Table 3) assuming that the flood height attenuation by friction over these areas is small. For the tidal wetlands, the higher vegetation canopy of the mangroves is expected to exert more friction and to result in higher storm surge height attenuation (10 cm/km) than the lower vegetation of salt marshes (8 cm/km) (Table 3). The remaining land area within the delta is considered as a unique land cover type, without discrimination in urban, forested or agricultural areas. It is assumed to have an average attenuation rate of 6 cm/km (Table 3). This value is based on the literature for hydrodynamic modelling of storm surge propagation over coastal low land areas (table 2) and on the assumption of a lower attenuation rate over human-developed land (typically dominated by agricultural land in deltas) than over natural wetlands. There

is much uncertainty about which precise values to use for these attenuation rates and how much they spatially vary. For this reason a sensitivity analysis was performed using a likely range of input values for the attenuation rates for these land cover types (see Table 3), showing that the model is relatively insensitive to it (see next section below).

Table 3 Storm surge attenuation rates attributed to the three land cover types considered in the study and used for the sensitivity analysis

Land cover type	Attenuation rate (cm/km)	Attenuation rates for the sensitivity analysis (cm/km)
Open water and Channels	0.1	
Mangrove	10.0	5, 10, 15, 20, 30, 40, 50
Salt Marsh	8.0	
Remaining land	6.0	4, 6, 8, 10, 15, 20

The model works as follows. A cost distance algorithm is applied over the delta to define the route that the storm surge follows during its landward propagation, i.e. the storm surge flood pathway. The cost distance algorithm defines the flood pathway between the flood source and every location (every pixel) of the delta system as the route where the traveling cost of the storm surge is the lowest based on the distance travelled and on the friction of the different land covers, or attenuation rates (Table 3). It then allocates the cost of traveling, i.e. the attenuation experienced by the storm surge, to every location. Subsequently, pixels where the resulting storm surge height is higher than the land elevation are considered at risk of flooding. The different steps of the model are presented for the example of the Ganges-Brahmaputra delta in India and Bangladesh (Fig.1).

The model produces two main outputs for storm surge return periods of 10, 100 and 1000 years:

(1) It identifies the areas within the delta, and the number of people living in those areas, that would be flooded via *flood pathways crossing tidal wetlands*. We assume that areas flooded via those routes would benefit more from nature-based attenuation of the storm surge, as compared to areas flooded via pathways that do not cross tidal wetlands. In order to select the pixels that are flooded or not flooded via tidal wetlands, two scenarios were compared. The first scenario represents the existing extent of tidal wetlands while the second scenario represents a situation where the tidal wetlands would be replaced by the remaining land cover type and its corresponding average attenuation rate (Table 3). Finally, all pixels with a higher storm surge attenuation for scenario 1 as compared to scenario 2 are identified as pixels having a storm surge pathway crossing tidal wetlands.

(2) It identifies the *length of the flood route crossing tidal wetlands* as a proxy for the magnitude of nature-based storm surge flood risk mitigation. We assume that the longer the flood wave travels through tidal wetlands before it reaches inhabited land, the more that flood wave will be attenuated. This was done by dividing the difference in storm surge levels between the two scenarios by the difference in attenuation rates of the tidal wetlands and remaining land (Table 3).

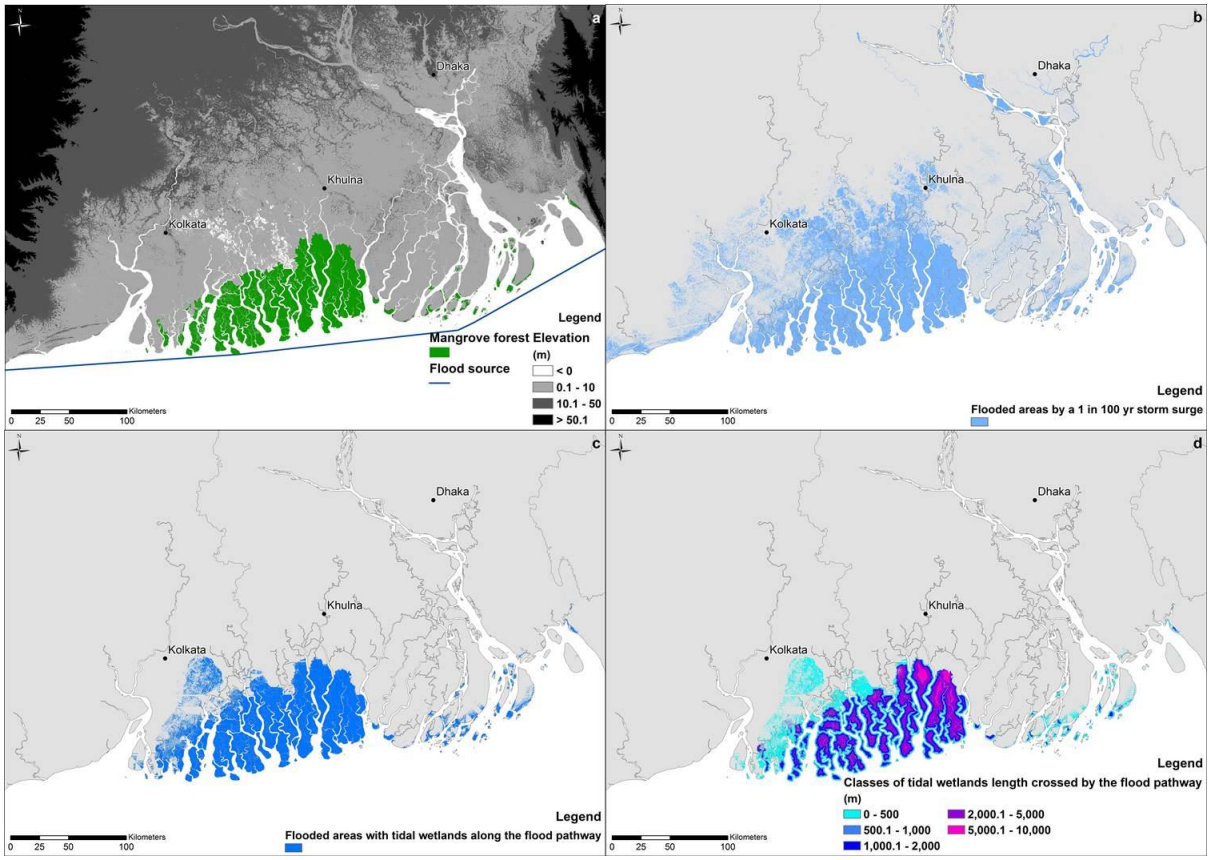

Fig. 1 Maps of the Ganges-Brahmaputra delta illustrating the steps of the model. (a)Input data: topography of the delta (meters above mean sea level), area of the mangrove forest and location of the source of the storm surge. (b) Estimated flood-prone areas for a 1 in 100 year storm surge accounting for different storm surge attenuation rates over mangroves, open water and land area (Table 3), i.e. scenario 1. (c) Flood-prone areas with a flood pathway passing through the mangrove forest. (d) Mangrove forest length along the flood pathway for every pixel classified into the five distance classes

Further, we introduced a measure for the relative magnitude of nature-based flood risk mitigation, which gives one value for the entire delta based on the length of the tidal wetlands along the flood pathways. This length is classified into distance classes *i*, which are classes of length of tidal wetlands along the flood pathway (see Table 4). The relative magnitude is calculated then in terms of land area (M_{land}) and population (M_{pop}) benefiting from nature-based flood risk mitigation from the following formula:

$$M = \sum \frac{N_i}{N} * W_i \quad (1)$$

Where M is the relative magnitude of the nature-based flood risk mitigation, N_i is the number of pixels or inhabitants in the distance class i, N is the total amount of pixels or inhabitants having a storm surge pathway crossing tidal wetlands and W is the weight of the distance class i (Table 4). The weight values follow a linear function based on the mean of each length class.

Table 4 Value of the weight (W) of each class of length of tidal wetlands along the flood pathway

Distance class (*i*)	Classes of tidal wetlands length along the flood pathway (m)	Mean length of the distance class (m)	Weight of the distance class (*W*)
1	0 – 500	250	1
2	500 – 1000	750	3
3	1000 – 2000	1500	6
4	2000 – 5000	3500	14
5	> 5000	7500	30

Sensitivity analysis

As the range of values for storm surge attenuation over land cover types underlie a certain variability in the literature, a sensitivity analysis on the Ganges-Brahmaputra delta (India and Bangladesh), i.e. the largest delta in our study, was performed to assess the dependence of our results to the chosen attenuation rates.

The tested parameters were the storm surge attenuation rate of the remaining land (4, 6, 8, 10, 15 and 20 cm/km) and of the tidal wetland area (in this case mangrove forest) (5, 10, 15, 20, 30, 40 and 50 cm/km) (Table 3).

Results

The results of the sensitivity analysis shows that the variation of the attenuation rates of the mangrove forest has a limited impact on the land area benefiting from storm surge mitigation by tidal wetlands, with averaged results of 1 812.60 km² ± 1.20 %; while the variation in the attenuation rates of the remaining land has a higher influence, with averaged results of 1 664.20 km² ± 12.80 % of land area benefiting from storm surge mitigation by tidal wetlands.

In the model, we assume one single value for the attenuation rate of the remaining land area, which is a simplification of the reality, as it is expected that the use of different attenuation rates for different land use types (urban area, fields, forests...) would have an impact on the propagation of the storm surge.

Nevertheless, the results of the sensitivity analysis suggest that the model output is robust in regards to the tested range of input values for the storm surge attenuation rates over the remaining land and tidal wetlands.

The results presented here after are for storm surges with a return period of 1 in 100 years. The results for the other return periods can be found in the Online Material and show qualitatively similar results.

Areas and populations benefiting from nature-based flood risk mitigation

Fig. 2 shows for each delta the land area (i.e. excluding the wetland areas themselves) and the population benefiting from flood risk mitigation by tidal wetlands, both in absolute numbers and in percentages. The percentages are expressed relative to the total land area or total population at risk of flooding within each delta for the current situation (scenario 1), i.e. the flood-exposed land area or population.

Considering the land area benefiting from flood risk mitigation by tidal wetlands, the response to the presence of tidal wetlands varies among deltas. In absolute numbers, the largest land areas buffered by

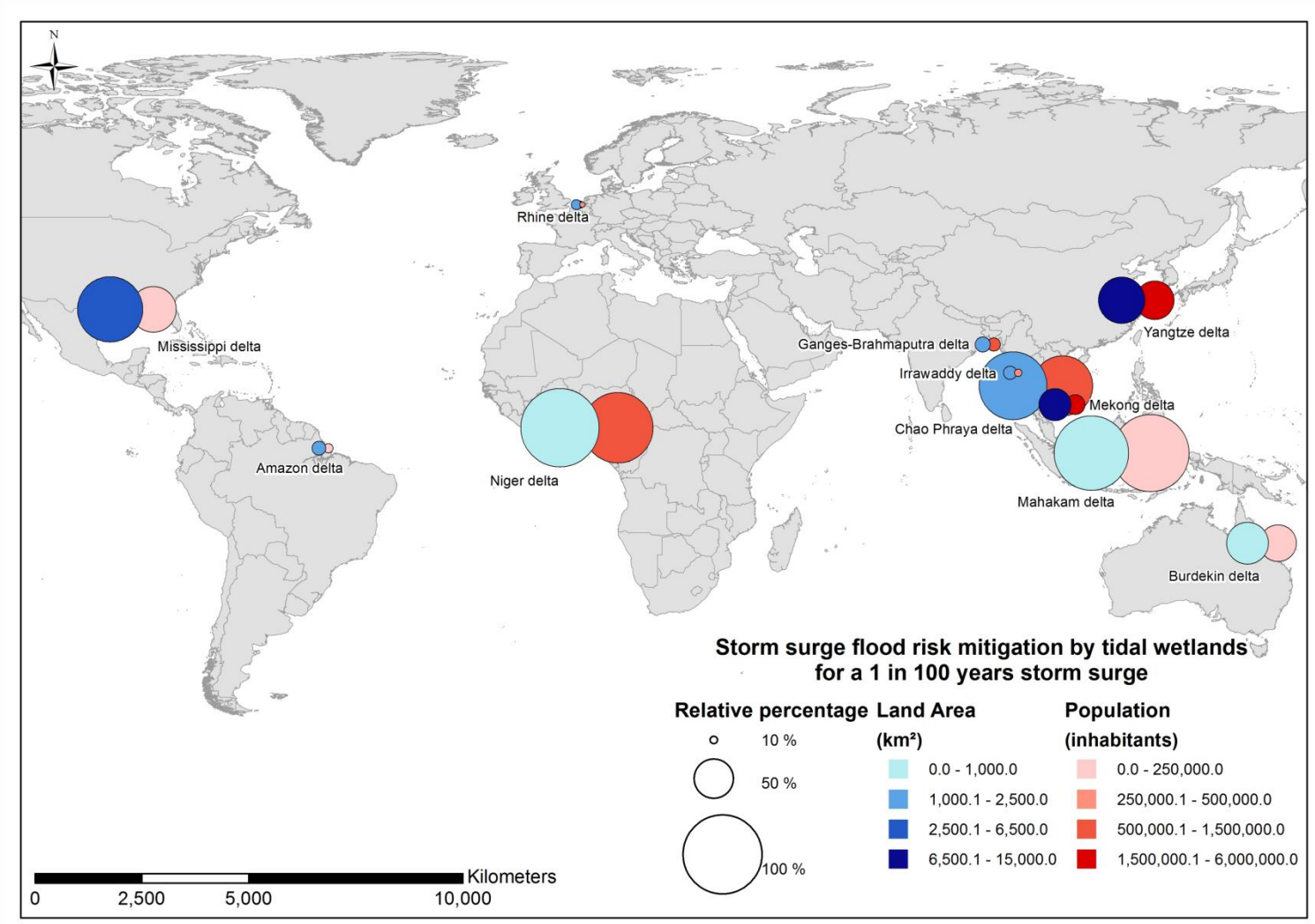

Fig. 2 Land surface area (left/blue) and number of people (right/red) benefiting from flood risk mitigation by tidal wetlands. The map represents the absolute land area (km²) or population (number of people) through the colour of the symbols, while the size represents the percentage of land area or population buffered by wetlands relative to flood-exposed land area or population

tidal wetlands are located in the Mekong (13 806 km²), Yangtze (9 229 km²) and Mississippi delta (4 407 km²), while the Burdekin (71 km²) represents the smallest land areas benefitting from nature-based flood risk mitigation (Fig. 3). Interestingly, this variation between deltas in total land area buffered by tidal wetlands is not correlated to the variation of the total tidal wetland area between deltas (Fig. 3, Pearson's r = - 0.073, p = 0.83). For example, the largest wetland areas are found in the Ganges-Brahmaputra (6 432 km²), Mississippi (6 015 km²) and Niger delta (5 647 km²), but these deltas do not represent the largest land areas buffered by tidal wetlands (Fig. 3). In terms of relative percentages, the Ganges-Brahmaputra, the Irrawaddy, the Amazon and the Rhine deltas, have about 15 to 20 % of their flood-exposed land area buffered by tidal wetlands. This percentage rises up to about 40 to 60 % for the Mekong, Burdekin and Yangtze deltas, while the other deltas present percentages of more than 80 % of the flood-exposed land area benefiting from flood risk mitigation by tidal wetlands.

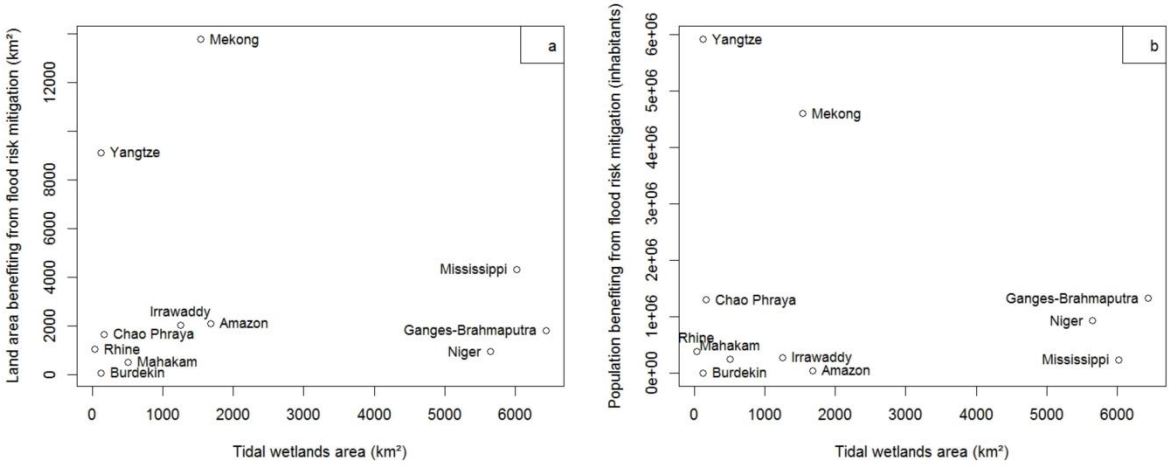

Fig. 3 (a) Relation between the land area benefiting from flood risk mitigation (km²) and the tidal wetlands surface area (km²) (Pearson's r = - 0.073; p = 0.83), (b) Relation between the population benefiting from flood risk mitigation (inhabitants) and the tidal wetlands surface area (km²) (Pearson's r = - 0.17, p = 0.61), for the 11 deltas studied

A similar pattern is found for the population buffered by tidal wetlands. In absolute numbers, the deltas with the highest number of inhabitants buffered by tidal wetlands are the Yangtze (5 922 009 inhabitants) and Mekong (4 602 641 inhabitants) delta, while the Burdekin delta is by far the delta with the lowest number of people (169 people) buffered by tidal wetlands. Also for the total population buffered by wetlands within a delta, there is no significant correlation to the total tidal wetland area within that delta (Pearson's r = -0.17, p = 0.61). In relative percentages, the Ganges-Brahmaputra, Irrawaddy, Amazon and Rhine deltas show the lowest percentages of flood-exposed population benefiting from flood risk mitigation by tidal wetlands (less than 20 %). The percentages of the Mekong, Burdekin, Yangtze and Mississippi deltas are of 25.4, 46.8, 49.1, and 58.1 % respectively, and the other deltas have more than 70 % of their flood-exposed population buffered by tidal wetlands, rising up to 98 % for the Mahakam delta.

Relative magnitude of the nature-based storm surge flood risk mitigation

The magnitude of the nature-based storm surge flood risk mitigation defined via the length of the flood pathway passing through tidal wetlands shows a large variability among deltas, with mean distances inside tidal wetlands ranging from 234 m to more than 2 km.

The comparison of the relative magnitude of nature-based flood risk mitigation is based on the magnitude *M* (eq. 1) in terms of land surface area (M_{land}) and delta population (M_{pop}) (Table 5). The magnitude is higher when a larger proportion of land area or population is buffered by a wider length of tidal wetlands.

Table 5 Value of the relative magnitude of nature-based flood risk mitigation in term of land area (M_{land}) and population (M_{pop}) for every delta

Delta	M_{land}	Ranking M_{land}	M_{pop}	Ranking M_{pop}
Ganges-Brahmaputra delta	6.26	3	1.53	9
Yangtze delta	1.07	11	1.02	11
Mekong delta	2.70	8	2.41	5
Chao Phraya delta	3.10	7	1.89	6
Irrawaddy delta	3.62	6	1.62	8
Niger delta	8.09	2	5.31	1
Amazon delta	4.47	4	2.95	4
Rhine delta	1.37	10	1.12	10
Mississippi delta	9.26	1	1.86	7
Mahakam delta	2.53	9	3.07	3
Burdekin delta	4.37	5	4.42	2

The relative magnitudes for land area range from 1.07 to 9.26 and for the delta population from 1.02 to 5.31. Except for the Mahakam and Burdekin deltas, all the deltas present higher magnitudes in terms of land area than in terms of population. However, the degree of deviation between M_{land} and M_{pop} varies among the deltas (Table 5). The Mississippi, Ganges-Brahmaputra and Niger deltas present the higher differences, while the Chao Phraya, Amazon and Irrawaddy deltas have smaller differences and the Yangtze, Burdekin, Rhine, Mekong and Mahakam present the lowest differences between M_{land} and M_{pop} (Fig. 4).

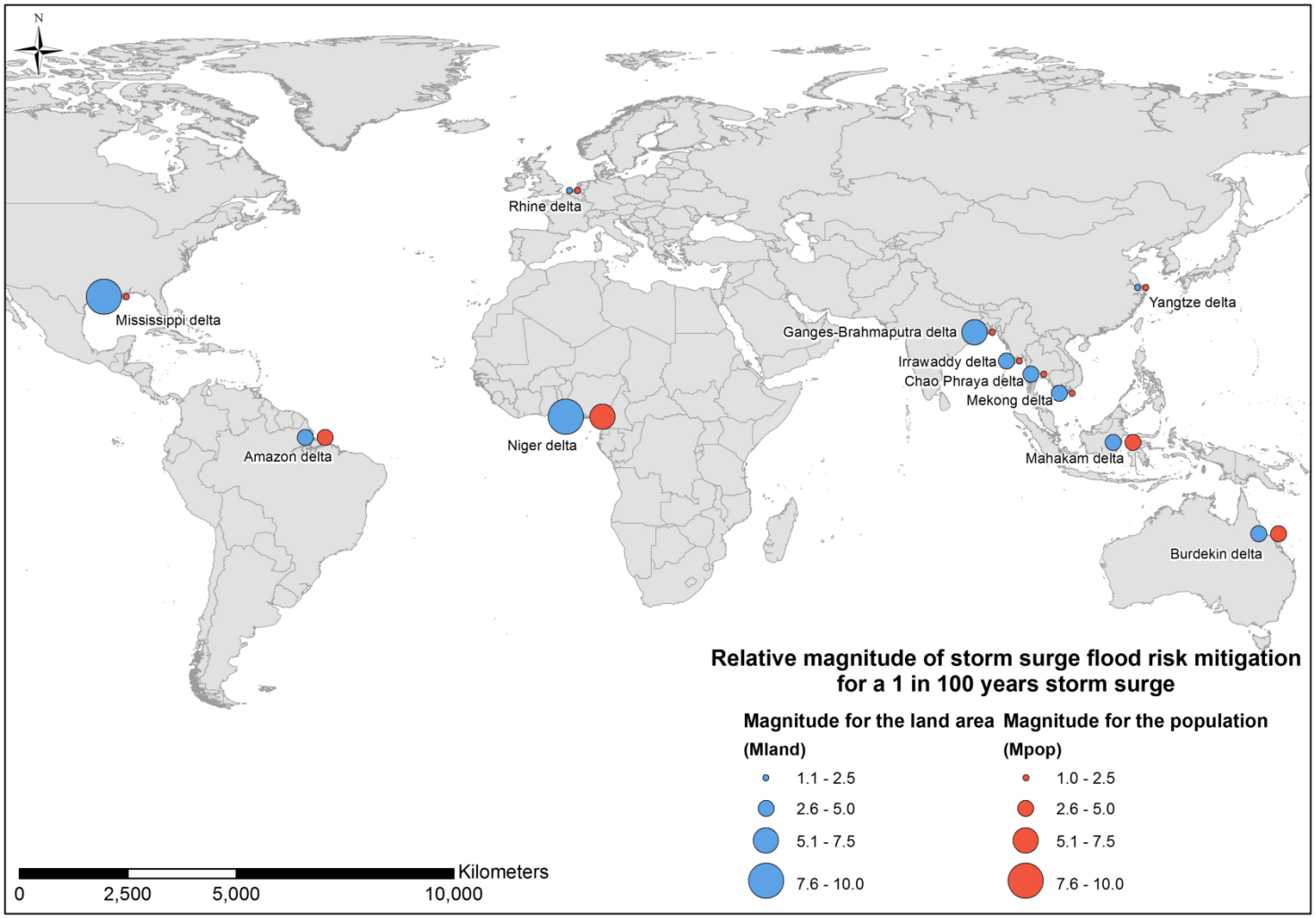

Fig. 4 Relative magnitude of nature-based storm surge flood risk mitigation for every delta in terms of land area (left/blue) and of population (right/red)

The comparison of the tidal wetlands area (km²) and the magnitude of flood risk mitigation for the land area (Fig. 5) shows a significant positive correlation (Pearson's r = 0.89, p = 0.0003). For an increasing tidal wetland area the magnitude of flood risk mitigation for the land increases. The correlation between the tidal wetlands area (km²) and the relative magnitude of flood risk mitigation for the population is non-significant (Pearson's r = 0.17, p = 0.61).

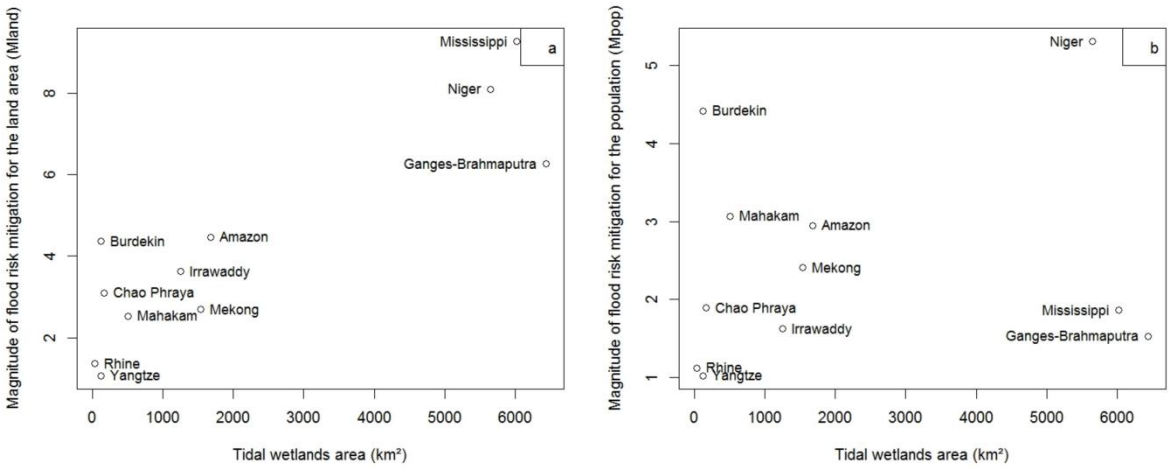

Fig. 5 (a) Relation between the tidal wetlands surface area (km²) and the relative magnitude of nature-based flood risk mitigation for the terrestrial land area (M_{land}) (Pearson's r = 0.88; p = 0.0003). (b) Relation between the tidal wetlands surface area (km²) and the relative magnitude of nature-based flood risk mitigation for the population (M_{pop}) (Pearson's r = 0.17; p = 0.61)

Discussion

Although nature-based coastal risk mitigation is rapidly gaining interest in the face of global change (Temmerman et al. 2013; Cheong et al. 2013; Spalding et al. 2014; Sutton-Grier et al. 2015; Giosan et al. 2014), current insights into the role of tidal wetlands for storm surge risk mitigation are mainly based on local or regional scale assessments (Costanza et al. 2008; Das and Vincent 2009; Wamsley et al. 2010; Zhang et al. 2012; Krauss et al. 2009; Stark et al. 2015), and methodologies for intermediate to global scale assessments are scarce. Our study contributes to fill this gap by developing a GIS model assessing the impact of the presence of tidal wetlands along the storm surge flood pathway in deltas around the world. We applied the model on 11 deltas, selected based on their population density, the presence of tidal wetlands and a worldwide distribution. Our results indicate that tidal wetlands provide storm surge mitigation to large percentages of the flood-exposed land area (> 80 %) for 4 of the 11 studied deltas, and to large percentages of the flood-exposed population (> 70 %) for 3 of the deltas. The land area and population buffered by tidal wetlands within a delta were not found to be correlated to the total wetland area in the delta, suggesting that more complex factors are at play, such as the spatial distribution of population within the delta, the delta geomorphology or the location of the tidal wetlands compared to the location of the population. The magnitude of the nature-based storm surge risk mitigation, estimated as the length of the storm surge pathway crossing tidal wetlands, was found to be significantly correlated to the tidal wetlands area within a delta. The latter finding highlights the importance of the conservation and, where possible, restoration of extensive continuous tidal wetland areas as a nature-based approach to mitigate storm surge flood risks in deltas.

Our quasi-global modelling approach differs from the existing complex hydrodynamic models applied in local to regional studies, which incorporate physical mechanisms of storm surge generation on the open sea, landward surge propagation and attenuation of peak surge levels by friction exerted by the landforms and vegetation of tidal wetlands and other coastal land use types (Resio and Westerink 2008; Wamsley et al. 2010; Zhang et al. 2012; Liu et al. 2013; Smolders et al. 2015; Haddad et al. 2016; Stark et al. 2016; Marsooli et al. 2016). Such hydrodynamic modelling approaches are data-demanding and computationally expensive, enabling their application on local to regional scales, but excluding their feasibility for application to many deltas worldwide. In contrast, our modelling approach is simple, computationally much less intensive, and based on input datasets that are globally available. As a first step, we demonstrated its applicability for 11 deltas, yet, the same approach is applicable to much more deltaic or non-deltaic areas around the world. The release of new global datasets is highly interesting, and such updated datasets should, when possible, be used in the future applications of our modelling approach. For example, there is the recently published global distribution of saltmarshes by McOwen et al. (2017) and the global dataset on storm surge levels by Muis et al. (2016).

The results presented highlight that our relatively simple method based on globally available data of generally lower resolution than local data can provide an estimation of the tidal wetland's capacity of risk mitigation at a regional scale. Nevertheless, despite the advantage of its intermediate to global applicability, our model, unlike hydrodynamic models, does not include parameters such as the complex geomorphology of the delta, the storm surge characteristics (such as storm intensity, duration, direction, forward moving speed) or the wetland characteristics (such as vegetation and geomorphic properties), making it unable to accurately predict the flooding extent, depth or duration as a result of a specific storm surge event.

Hence, a direct comparison between hydrodynamic models and our GIS model is not very informative as the methods represent different conditions in their simulations. Hydrodynamic models are setup for specific storm surge characteristics, including specific wind velocity fields, storm track, duration etc., with typical output being among others the reduction of peak storm surge height due to the presence of tidal wetlands (Wamsley et al. 2010; Zhang et al. 2012). Whereas our GIS model is setup for 'statistical' storm surge height of a given return period, neglecting the specific storm surge characteristics mentioned above, and aims to identify the land area and population that is exposed to flood risks via flood pathways crossing tidal wetlands and that will benefit from reduced flood risks due to the presence of the tidal wetlands. . Nevertheless, a number of qualitative conclusions derived from both modelling approaches are comparable, as discussed below.

The analysis of the sensitivity of the model output to the variation of the input values for attenuation rates for the land area (1 664.20 km² ± 12.80 %) and for the tidal wetlands (i.e. mangrove forests) (1 812.60 km² ± 1.2 %) reveals that the model is robust in regards to those parameters. The reason why the model output (i.e. the land area flooded via flood pathways crossing through tidal wetlands) is relatively insensitive to the wetland attenuation rates that are applied can be ascribed to two points. First, a main point explaining this low variation of the land area benefiting from storm surge mitigation by tidal wetlands is the continuity or connectivity of the tidal wetlands. A tidal wetland area dissected by channels, embayment and land areas will introduce a non-linear parameter in the reduction of the surge, as it will not only be related to the attenuation rate of the wetlands, but also to the pathway the flood can follow. Because a higher attenuation rate is applied for the wetlands compared to water and other land surfaces, the flood will preferably propagate over areas of lower friction, such as the channels and land areas. As a result, the area benefiting from flood risk mitigation by tidal wetlands is relatively insensitive to the range of attenuation rates that were applied in our

sensitivity analysis (5 to 50 cm/km), as channels and land areas in between wetland areas will remain the main pathways of flood propagation.

The second point is related to the different land use classes. In the current design of the model, the land area is divided into two classes, the tidal wetlands and the other land area, whilst, the division of the land area into an increased number of classes (e.g. forests, urban areas, agricultural fields...) is expected to modify and refine the pathway of the storm surge in the delta area.

Our analysis shows that there is no correlation between the surface area of the delta's tidal wetlands and the land area benefiting from storm surge mitigation. This is corroborating the fact that even small wetlands can provide flood wave attenuation to large areas (Gedan et al. 2011). The comparison of the Ganges-Brahmaputra and the Chao Phraya deltas further illustrates this. The Ganges-Brahmaputra delta has a total surface area of tidal wetlands of 6 432 km² that provides flood risk mitigation to 1 821 km² of the delta area. In comparison, the Chao Phraya delta has 174 km² of tidal wetlands and 1 666 km² of land area benefiting from nature-based flood risk mitigation. The non-correlation between the wetlands surface area and the land area benefiting from storm surge mitigation can also be related to the effect of the tidal wetlands location in the delta and along the channels that is known to influence their capacity to mitigate storm surges (Smolders et al. 2015; Stark et al. 2015). Following the previous example of the Ganges-Brahmaputra and Chao Phraya deltas, the effect of the location of the tidal wetlands in the delta can be observed. Tidal wetlands of the Chao Phraya delta are more scattered and present along the main channels of the delta (see maps of the deltas in Online Material), which implies that they influence the propagation of the flood wave for a large part of the delta (1 666 km²). In contrast, tidal wetlands of the Ganges-Brahmaputra delta are clustered, leaving some of the main channels, such as the ones running to Kolkata or Dhaka for example, exempt of tidal wetlands. Hence, the large tidal wetland area within the Ganges-Brahmaputra delta (i.e. the Sundarbans mangrove forest) provides nature-based flood risk mitigation to only a certain part (1 821 km²) of this large deltaic area.

Nevertheless, the analysis shows a significant, positive correlation between the surface area of tidal wetlands and the magnitude of nature-based storm surge risk mitigation (Pearson's $r = 0.88$, p-value = 0.0003). This implies that a delta with a large and/or continuous surface area occupied by tidal wetlands will benefit from a higher magnitude of flood risk mitigation due to a longer width of tidal wetlands crossed by the flood pathway. This finding relates to several hydrodynamic studies that have identified the importance of wetland continuity for effective attenuation of storm surges (Phan et al. 2015; Mcivor et al. 2012; Zhang et al. 2012; Loder et al. 2009).

In addition, studies have pointed out that tidal wetlands dissected by deep and wide channels provide less storm surge attenuation than wetlands with narrow and shallow channels (Loder et al. 2009; Stark et al. 2016). On the large scale of a delta area, our results show similar effects of the dissection of the tidal wetlands by deltaic channels. A qualitative observation of the studied deltas shows that the deltas having the lower relative magnitude of nature-based risk mitigation are also the deltas having large channels dissecting the wetlands, as for example the Rhine or the Yangtze deltas.

When a delta has a high value of land area benefiting from flood risk mitigation, like the 86 % of the Chao Phraya delta or the 95 % of the Mahakam delta, this does not necessarily imply a high magnitude of storm surge flood risk mitigation. The M_{land} of the Chao Phraya and Mahakam deltas are 3.10 and 2.53 respectively, almost three times lower than the magnitude of the Mississippi or the Niger deltas. This means that although the Chao Phraya and Mahakam deltas have a high land area benefiting from flood risk mitigation by tidal wetlands, the magnitude of the mitigation is rather small

compared to the magnitude estimated for the Mississippi or Niger delta for which the flood pathway is crossing in general a longer width of tidal wetlands.

Neither the absolute number of people buffered by tidal wetlands nor the relative magnitude of nature-based storm surge mitigation in terms of population is correlated to the total tidal wetlands area in the delta, implying that other parameters must be considered. This may be attributed to factors such as the spatial population distribution and density, or the historical settlement of the population and their spatial relation to tidal wetlands. The Niger, Burdekin and Mahakam deltas have the population benefitting from the highest magnitude of storm surge risk mitigation in terms of population, with values of 5.31, 4.42 and 3.07 respectively. The tidal wetlands in those deltas are located in between the population and the sea and are present over the full extent of the coastline. They differ in population distribution, as the population of the Niger delta is distributed over the delta plain, while the population of the Mahakam and Burdekin deltas is concentrated in cities. However, the presence of tidal wetlands along the coastline and along either side of the channels is influencing the propagation of the flood pathway that crosses the tidal wetlands before reaching the population located behind. Those deltas are in contrast to other deltas, such as the Yangtze and Rhine deltas, where the channels are wider, with smaller tidal wetlands located only in some regions of the delta; or to the Ganges-Brahmaputra delta, where the tidal wetlands occupy a large portion of the delta, but a large part of the population is not located directly behind the wetlands resulting in a lower magnitude in term of population.

Ranking the deltas according to the relative magnitude of storm surge mitigation in terms of land area, demonstrates that the deltas with the highest ranking are deltas where large tidal wetlands exist and where historic wetland reclamation and conversion into human land use has been limited, such as in the Mississippi, Niger and Ganges-Brahmaputra deltas (Table 5). In contrast, the deltas with the lowest ranking have experienced large scale historical wetland reclamation, such as in the Yangtze and Rhine delta. Hence, the difference in historical land use management of the deltas induces differences in the future management. Deltas with limited wetland reclamation and large remaining wetlands, such as the Mississippi, Niger and Ganges-Brahmaputra delta would benefit from investing in the conservation of their tidal wetlands as a nature-based strategy to mitigate storm surge flood risks, while deltas with extensive historical wetland reclamation, such as the Yangtze and Rhine deltas, should not only rely on hard engineering of flood defence structures but also invest in restoration of formerly reclaimed wetlands where possible.

Acknowledgements

The author would like to thank the different data providers and Dr. Chen Wang for her help in the gathering of the Chinese wetlands data. This work was funded by the University of Antwerp.

References

Arkema, Katie K., Greg Guannel, Gregory Verutes, Spencer a. Wood, Anne Guerry, Mary Ruckelshaus, Peter Kareiva, Martin Lacayo, and Jessica M. Silver. 2013. Coastal habitats shield people and property from sea-level rise and storms. *Nature Climate Change* 3:913-918. doi:10.1038/nclimate1944.

Barbier, Edward B., Ioannis Y. Georgiou, Brian Enchelmeyer, and Denise J. Reed. 2013. The Value of Wetlands in Protecting Southeast Louisiana from Hurricane Storm Surges. *PLoS ONE* 8:1-6. doi:10.1371/journal.pone.0058715.

Bengtsson, Lennart, Kevin I. Hodges, and Erich Roeckner. 2006. Storm Tracks and Climate Change. *Journal of Climate* 19:3518-3543. doi:10.1175/JCLI3815.1.

Bright, Eddie A, Phil R Coleman, Amy N Rose, and Marie L Urban. 2013. LandScan 2013. Oak Ridge, TN: Oak Ridge National Laboratory SE - July 1, 2012.

Cheong, So-Min, Brian Silliman, Poh Poh Wong, Bregje van Wesenbeeck, Choong-Ki Kim, and Greg Guannel. 2013. Coastal adaptation with ecological engineering. *Nature Climate Change* 3:787-791. doi:10.1038/nclimate1854.

Costanza, Robert, Octavio Pérez-Maqueo, M Luisa Martinez, Paul Sutton, Sharolyn J Anderson, and Kenneth Mulder. 2008. The value of coastal wetlands for hurricane protection. *Ambio* 37:241-248. doi:10.1579/0044-7447(2008)37[241:tvocwf]2.0.co;2.

Das, Saudamini, and Jeffrey R Vincent. 2009. Mangroves protected villages and reduced death toll during Indian super cyclone. *Proceedings of the National Academy of Sciences of the United States of America* 106:7357-7360. doi:10.1073/pnas.0810440106.

Dasgupta, Susmita, Benoit Laplante, Siobhan Murray, and David Wheeler. 2011. Exposure of developing countries to sea-level rise and storm surges. *Climatic Change* 106:567-579. doi:10.1007/s10584-010-9959-6.

Day, John W, Donald F Boesch, Ellis J Clairain, G Paul Kemp, Shirley B Laska, William J Mitsch, Kenneth Orth et al. 2007. Restoration of the Mississippi Delta: lessons from Hurricanes Katrina and Rita. *Science (New York, N.Y.)* 315:1679-1684. doi:10.1126/science.1137030.

Dobson, Jerome E., Edward A. Bright, Phillip R. Coleman, Richard C. Durfee, and Brian A. Worley. 2000. LandScan: A global population database for estimating populations at risk. *Photogrammetric Engineering and Remote Sensing* 66:849-857.

Duarte, Carlos M., Iñigo J. Losada, Iris E. Hendriks, Inés Mazarrasa, and Núria Marbà. 2013. The role of coastal plant communities for climate change mitigation and adaptation. *Nature Climate Change* 3:961-968. doi:10.1038/nclimate1970.

Ericson, J, C Vorosmarty, S Dingman, L Ward, and M Meybeck. 2006. Effective sea-level rise and deltas: Causes of change and human dimension implications. *Global and Planetary Change* 50:63-82. doi:10.1016/j.gloplacha.2005.07.004.

Federal Geographic Data Committee. 2013. Classification of wetlands and deepwater habitats of the United States. In *FGDC-STD-004-2013. Second Edition*. Washington D.C.: Wetlands Subcommittee, Federal Geographic Data Committee and U.S. Fish and Wildlife Service.

Gedan, Keryn B., Matthew L. Kirwan, Eric Wolanski, Edward B. Barbier, and Brian R. Silliman. 2011. The present and future role of coastal wetland vegetation in protecting shorelines: Answering recent challenges to the paradigm. *Climatic Change* 106:7-29. doi:10.1007/s10584-010-0003-7.

Giosan, Liviu, James P.M. Syvitski, Stefan Constantinescu, and John Day. 2014. Protect the world's deltas. *Nature* 516:31-33.

Giri, C., E. Ochieng, L. L. LL Tieszen, Z. Zhu, A. Singh, T. Loveland, J. Masek, N. Duke, and Duke N. 2011. Status and distribution of mangrove forests of the world using earth observation satellite data. *Global Ecology and Biogeography* 20:154-159. doi:10.1111/j.1466-8238.2010.00584.x.

Haddad, Jana, Seth Lawler, and Celso M. Ferreira. 2016. Assessing the relevance of wetlands for storm surge protection: a coupled hydrodynamic and geospatial framework. *Natural Hazards* 80:839-861. doi:10.1007/s11069-015-2000-7.

Hallegatte, Stéphane, Colin Green, Robert J. Nicholls, and Jan Corfee-Morlot. 2013. Future flood losses in major coastal cities. *Nature Climate Change* 3:802-806. doi:10.1038/nclimate1979.

Heap, A, S Bryce, D Ryan, L Radke, C Smith, R Smith, P Harris, and D Heggie. 2001. Australian estuaries & coastal waterways: a geoscience perspective for improved and integrated resource management. In *Australian Geological Survey Organisation*.

Hinkel, Jochen, Daniel Lincke, Athanasios T Vafeidis, Mahé Perrette, Robert James Nicholls, Richard S J Tol, Ben Marzeion, Xavier Fettweis, Cezar Ionescu, and Anders Levermann. 2014. Coastal flood damage and adaptation costs under 21st century sea-level rise. *Proceedings of the National Academy of Sciences of the United States of America* 111:3292-3297. doi:10.1073/pnas.1222469111.

Kirwan, Matthew L., Stijn Temmerman, Emily E. Skeehan, Glenn R. Guntenspergen, and Sergio Faghe. 2016. Overestimation of marsh vulnerability to sea level rise. *Nature Climate Change* 6:253-260. doi:10.1038/nclimate2909.

Krauss, Ken W., Terry J. Thomas W. Doyle, Terry J. Thomas W. Doyle, Christopher M. Swarzenski, Andrew S. From, Richard H. Day, and William H. Conner. 2009. Water level observations in mangrove swamps during two hurricanes in Florida. *Wetlands* 29:142-149. doi:10.1672/07-232.1.

Lichter, Michal, Athanasios T. Vafeidis, Robert J. Nicholls, and Gunilla Kaiser. 2011. Exploring data-related uncertainties in analyses of land area and population in the "Low-Elevation Coastal Zone" (LECZ). *Journal of Coastal Research* 27 (4):757-768. doi:10.2112/JCOASTRES-D-10-00072.1.

Liu, Huiqing, Keqi Zhang, Yuepeng Li, and Lian Xie. 2013. Numerical study of the sensitivity of mangroves in reducing storm surge and flooding to hurricane characteristics in southern Florida. *Continental Shelf Research* 64:51-65. doi:10.1016/j.csr.2013.05.015.

Loder, N. M., J. L. Irish, M. a. Cialone, and T. V. Wamsley. 2009. Sensitivity of hurricane surge to morphological parameters of coastal wetlands. *Estuarine, Coastal and Shelf Science* 84:625-636. doi:10.1016/j.ecss.2009.07.036.

Lovelace, John K. 1994. Storm-Tide Elevations Produced By Hurricane Andrew Along the Louisiana Coast, August 25-27,1992. *U.S. Geological Survey Open-File Report 94-371. Prepared in cooperation with the Federal Emergency Management Agency.*

Marsooli, Reza, Philip M Orton, Nickitas Georgas, and Alan F Blumberg. 2016. Three-dimensional hydrodynamic modeling of coastal fl ood mitigation by wetlands. *Coastal Engineering* 111:83-94. doi:10.1016/j.coastaleng.2016.01.012.

McGee, Benton D., Burl B. Goree, Roland W. Tollett, Brenda K. Woodward, and Wade H. Kress. 2006. Hurrican Rita Surge Data, Southwestern Louisiana and Souteasthern Texas, September to November 2005. *U.S. Geological Survey Data Series 220*.

McGranahan, G., D. Balk, and B. Anderson. 2007. The rising tide: assessing the risks of climate change and human settlements in low elevation coastal zones. *Environment and Urbanization* 19:17-37. doi:10.1177/0956247807076960.

Mcivor, Anna, Tom Spencer, Iris Möller, and Mark Spalding. 2012. Storm Surge Reduction by Mangroves. *Natural Coastal Protection Series*:35.

Mcowen, Chris, Lauren Weatherdon, Jan-Willem Bochove, Emma Sullivan, Simon Blyth, Christoph Zockler, Damon Stanwell-Smith et al. 2017. A global map of saltmarshes. *Biodiversity Data Journal* 5:e11764. doi:10.3897/BDJ.5.e11764.

Muis, Sanne, Martin Verlaan, Hessel C. Winsemius, Jeroen C. J. H. Aerts, and Philip J. Ward. 2016. A global reanalysis of storm surges and extreme sea levels. *Nature Communications* 7:11969. doi:10.1038/ncomms11969.

Neumann, Barbara, Athanasios T. Vafeidis, Juliane Zimmermann, and Robert J. Nicholls. 2015. Future Coastal Population Growth and Exposure to Sea-Level Rise and Coastal Flooding - A Global Assessment. *PLoS ONE* 10:e0118571. doi:10.1371/journal.pone.0118571.

Niu, Zhen Guo, Peng Gong, Xiao Cheng, Jian Hong Guo, Lin Wang, Hua Bing Huang, Shao Qing Shen et al. 2009. Geographical characteristics of China's wetlands derived from remotely sensed data. *Science in China, Series D: Earth Sciences* 52:723-738. doi:10.1007/s11430-009-0075-2.

Phan, Linh K, Jaap S. M. van Thiel de Vries, and Marcel J F Stive. 2015. Coastal Mangrove Squeeze in the Mekong Delta. *Journal of Coastal Research* 31:233-243. doi:10.2112/JCOASTRES-D-14-00049.1.

Resio, Donald T., and Joannes J. Westerink. 2008. Modeling the physics of storm surges. *Physics Today* 61:33-38. doi:10.1063/1.2982120.

Rodriguez, E, C. Cs Morris, and J. Je Belz. 2006. A global assessment of the SRTM performance. *Photogrammetric Engineering and Remote Sensing* 72:249-260. doi:10.14358/PERS.72.3.249.

Shepard, Christine C., Caitlin M. Crain, and Michael W. Beck. 2011. The protective role of coastal marshes: A systematic review and meta-analysis. *PLoS ONE* 6. doi:10.1371/journal.pone.0027374.

Small, Christopher, and Robert J Nicholls. 2003. A Global Analysis of Human Settlement in Coastal Zones. *Journal of Coastal Research* 19:584-599.

Smolders, S., Y. Plancke, S. Ides, P. Meire, and S. Temmerman. 2015. Role of intertidal wetlands for tidal and storm tide attenuation along a confined estuary: a model study. *Natural Hazards and Earth System Sciences Discussions* 3:3181-3224. doi:10.5194/nhessd-3-3181-2015.

Spalding, M., Anna Mcivor, FH. Tonneijck, S. Tol, and P. van Eijk. 2014. Mangroves for coastal defence. Guidelines for coastal managers & policy makers.

Stark, J., T. Van Oyen, P. Meire, and S. Temmerman. 2015. Observations of tidal and storm surge attenuation in a large tidal marsh. *Limnology and Oceanography*:n/a-n/a. doi:10.1002/lno.10104.

Stark, Jeroen, Yves Plancke, Stefaan Ides, Patrick Meire, and Stijn Temmerman. 2016. Coastal flood protection by a combined nature-based and engineering approach: Modeling the effects of marsh geometry and surrounding dikes. *Estuarine, Coastal and Shelf Science* 175:34-45. doi:10.1016/j.ecss.2016.03.027.

Sun, G., K. J. Ranson, V. I. Kharuk, and K. Kovacs. 2003. Validation of surface height from shuttle radar topography mission using shuttle laser altimeter. *Remote Sensing of Environment* 88:401-411. doi:10.1016/j.rse.2003.09.001.

Sutton-Grier, Ariana E., Kateryna Wowk, and Holly Bamford. 2015. Future of our coasts: The potential for natural and hybrid infrastructure to enhance the resilience of our coastal communities, economies and ecosystems. *Environmental Science and Policy* 51:137-148. doi:10.1016/j.envsci.2015.04.006.

Temmerman, Stijn, and Matthew L. Kirwan. 2015. Building land with a rising sea. *Science* 349:588-589.

Temmerman, Stijn, Patrick Meire, Tjeerd J Bouma, Peter M J Herman, Tom Ysebaert, and Huib J De Vriend. 2013. Ecosystem-based coastal defence in the face of global change. *Nature* 504:79-83. doi:10.1038/nature12859.

Tessler, Z. D., C. J. Vörösmarty, M. Grossberg, I. Gladkova, H. Aizenman, J. P. M. Syvitski, and E. Foufoula-Georgiou. 2015. Profiling risk and sustainability in coastal deltas of the world. *Science* 349:638-643.

United States Army Corps of Engineers. 2006. Louisiana coastal protection and restoration (LaCPR) preliminary technical report to United States Congress.

UT BATTELLE LLC. LandScan frequently asked questions. Developed under Prime Contract No. DE-AC05-00OR22725 with the U.S. Department of Energy. The U.S. Government has certain rights herein. http://web.ornl.gov/sci/landscan/landscan_faq.shtml. Accessed 2016.

Vafeidis, Athanasios T., G. Boot, J. Cox, L. Mcfadden, and R.J. Nicholls. 2005. The diva database documentation.1-33.

Wamsley, Ty V., Mary A. Cialone, Jane M. Smith, John H. Atkinson, and Julie D. Rosati. 2010. The potential of wetlands in reducing storm surge. *Ocean Engineering* 37:59-68. doi:10.1016/j.oceaneng.2009.07.018.

Woodruff, Jonathan D, Jennifer L Irish, and Suzana J Camargo. 2013. Coastal flooding by tropical cyclones and sea-level rise. *Nature* 504:44-52. doi:10.1038/nature12855.

Zhang, Keqi, Huiqing Liu, Yuepeng Li, Hongzhou Xu, Jian Shen, Jamie Rhome, and Thomas J. Smith. 2012. The role of mangroves in attenuating storm surges. *Estuarine, Coastal and Shelf Science* 102-103:11-23. doi:10.1016/j.ecss.2012.02.021.

Supplementary Online Material
Contribution of mangroves and salt marshes to nature-based mitigation of coastal flood risks in major deltas of the world

R. Van Coppenolle[1], C. Schwarz[2], S. Temmerman[1]

[1] Ecosystem Management Research Group, Department of Biology, University of Antwerp, Universiteitsplein 1C, 2610 Wilrijk, Belgium
[2] Coastal Research Group, Department of Physical Geography, Faculty of Geosciences, Utrecht University, P.O. Box 80115, 3508 TC Utrecht, the Netherlands

Corresponding author: Rebecca Van Coppenolle, E-mail: rebecca.vancoppenolle@uantwerpen.be, phone: 0032 3 265 87 12

1. Supplementary information on the deltas

Ganges-Brahmaputra delta, India and Bangladesh

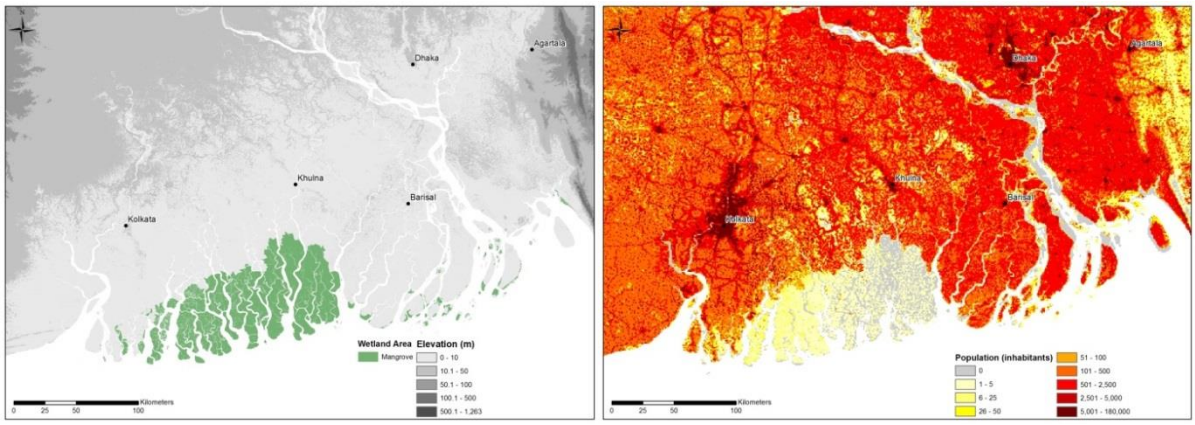

Fig S1 Left: Topography and location of the tidal wetlands in the Ganges-Brahmaputra delta in India and Bangladesh. Right: Ambient population in the delta

Yangtze delta, China

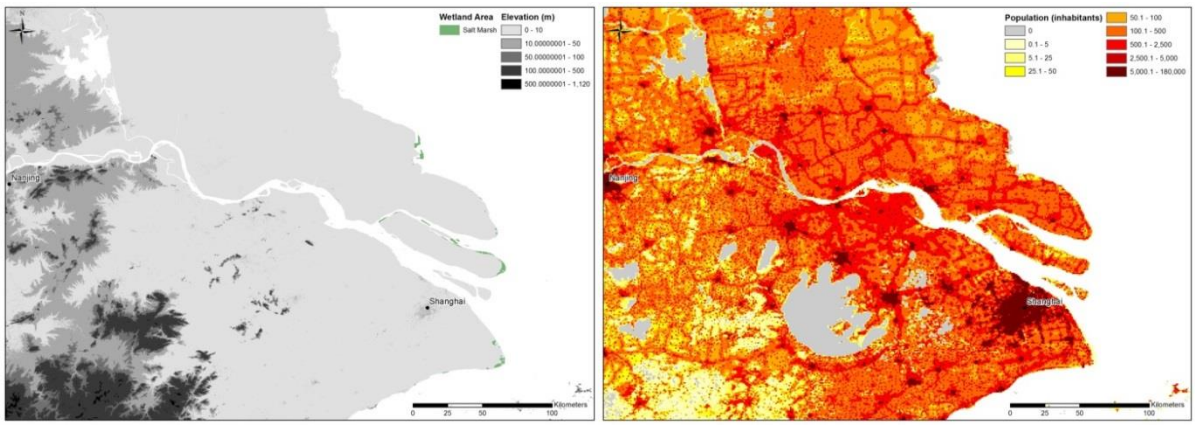

Fig S2 Left: Topography and location of the tidal wetlands in the Yangtze delta in China. Right: Ambient population in the delta

Mekong delta, Vietnam

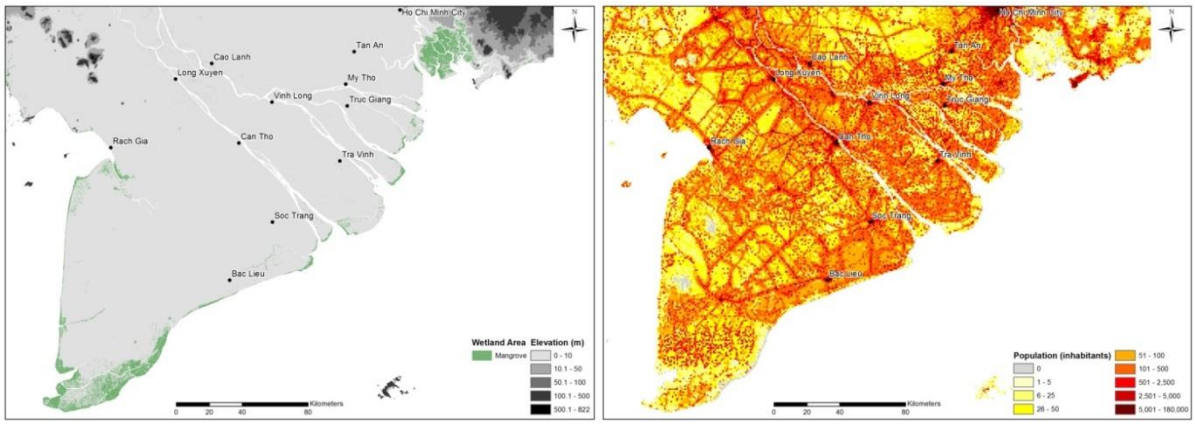

Fig S3 Left: Topography and location of the tidal wetlands in the Mekong delta in Vietnam. Right: Ambient population in the delta

Chao Phraya delta, Thailand

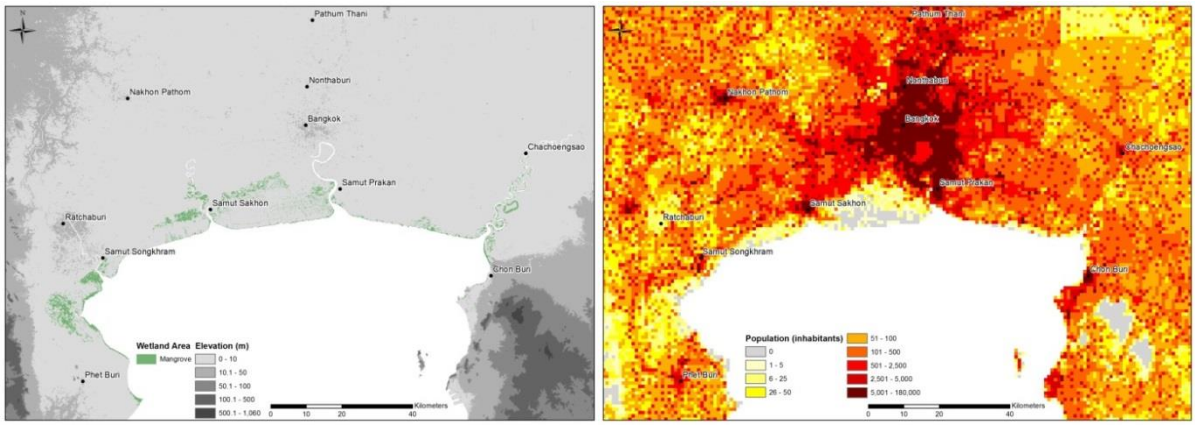

Fig S4 Left: Topography and location of the tidal wetlands in the Chao Praya delta in Thailand. Right: Ambient population in the delta

Irrawaddy delta, Myanmar

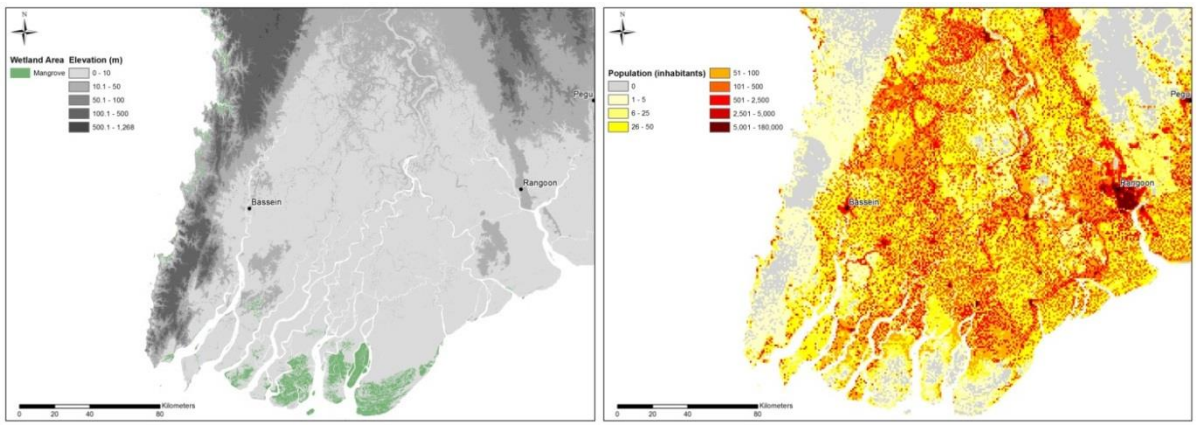

Fig S5 Left: Topography and location of the tidal wetlands in the Irrawaddy delta in Myanmar. Right: Ambient population in the delta

Niger delta, Nigeria

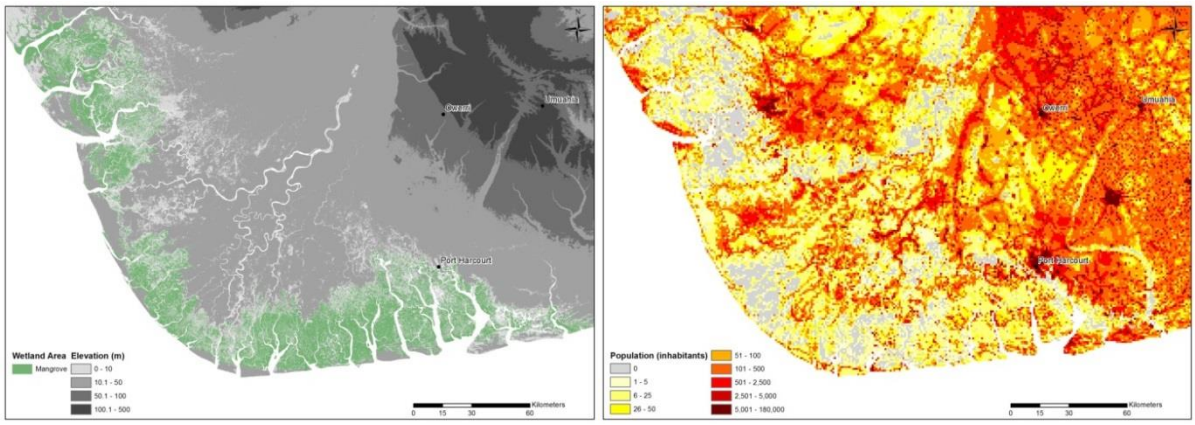

Fig S6 Left: Topography and location of the tidal wetlands in the Niger delta in Nigeria. Right: Ambient population in the delta

Amazon delta,Brazil

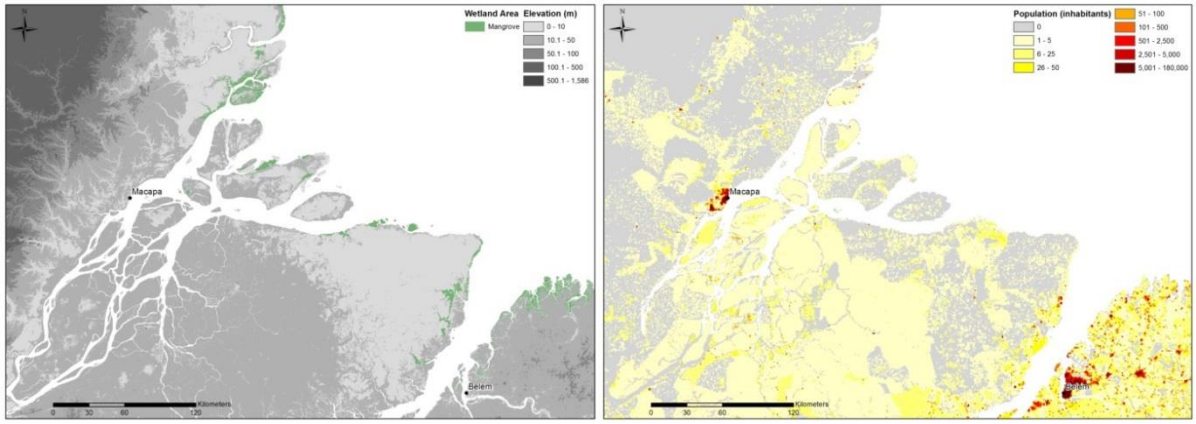

Fig S7 Left: Topography and location of the tidal wetlands in the Amazon delta in Brazil. Right: Ambient population in the delta

Rhine delta, The Netherlands

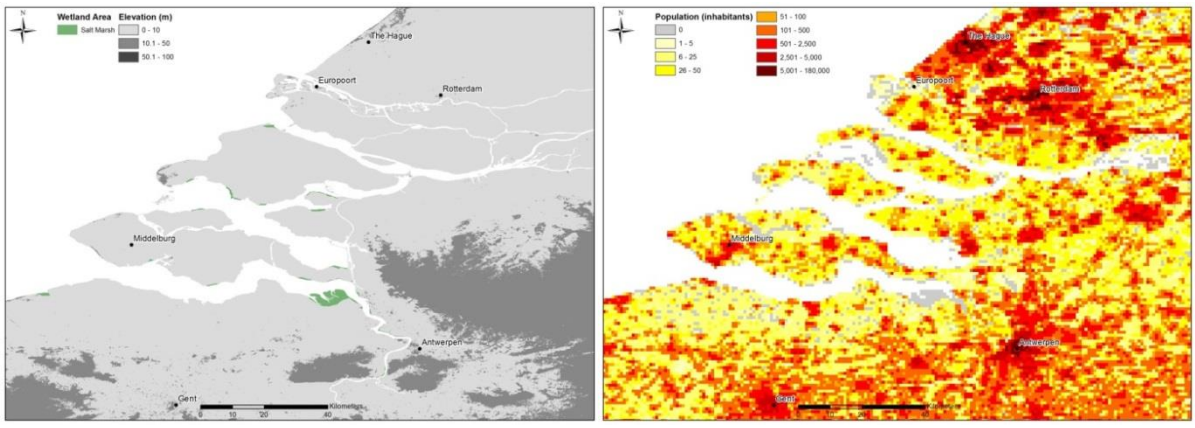

Fig S8 Left: Topography and location of the tidal wetlands in the Rhine delta in The Netherlands. Right: Ambient population in the delta

Mississippi delta, United States of America

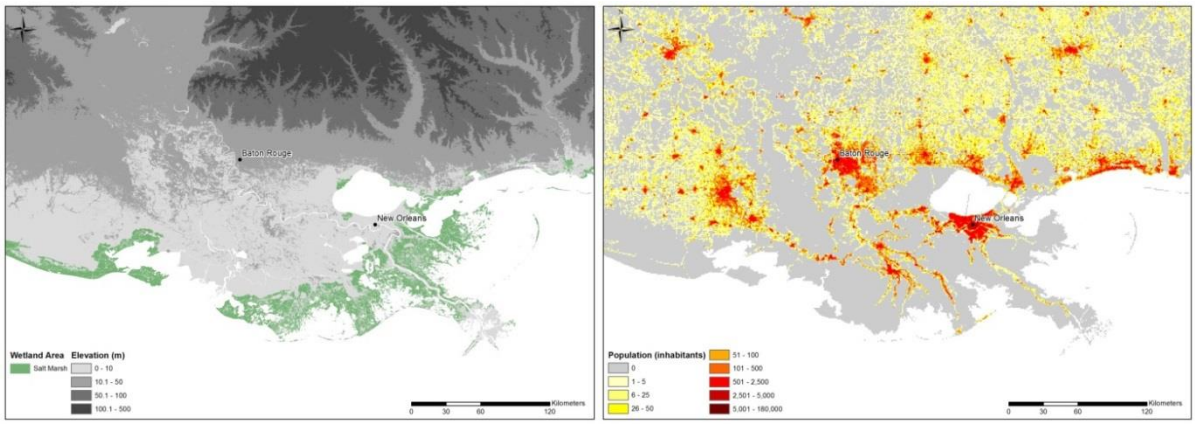

Fig S9 Left: Topography and location of the tidal wetlands in the Mississippi delta in the USA Right: Ambient population in the delta

Mahakam delta, Indonesia

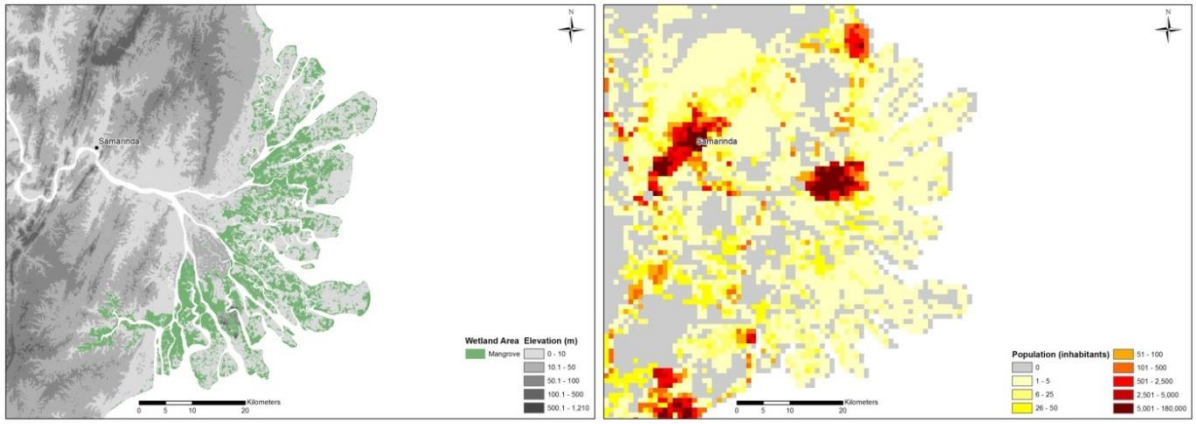

Fig S10 Left: Topography and location of the tidal wetlands in the Mahakam delta in Indonesia. Right: Ambient population in the delta

Burdekin delta, Australia

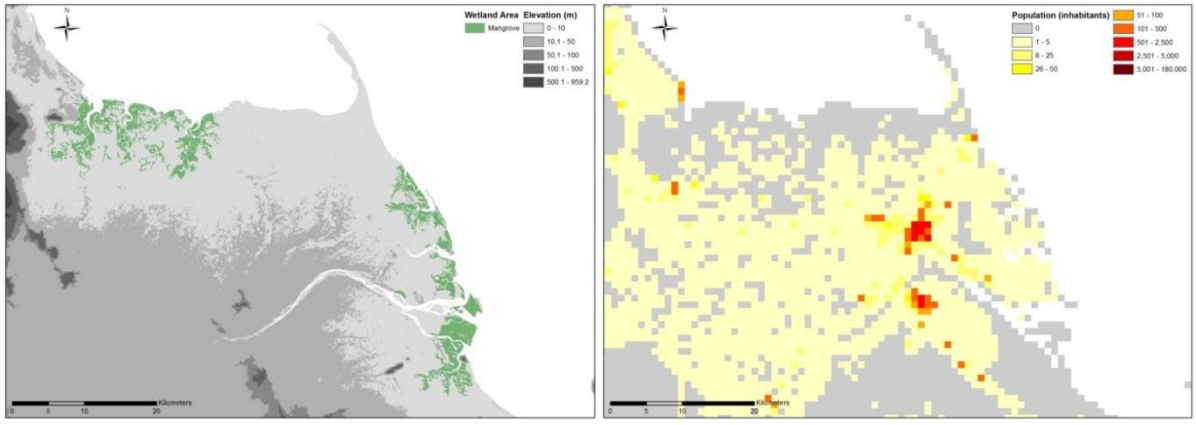

Fig S11 Left: Topography and location of the tidal wetlands in the Burdekin delta in Australia. Right: Ambient population in the delta

2. Supplementary explanation on the DIVA dataset

The DIVA coastline is based on the coastline of the Digital Chart of the World (DCW, Environmental Systems Research Institute, ESRI, 2002) and stores the values of storm surge height for every segment of the coastline and for several return periods.

In the study, the origin of the storm surge was defined as a flood source (red line in Figure S12) and the value of the storm surge heights was transferred to this flood source via a Euclidean distance algorithm. The Euclidean distance algorithm delineated for every segment of the DIVA coastline its area of influence (thin black lines in Figure S12). Then, the flood source was segmented and the value of every segment corresponds to the value of the area of influence in which the segment is located.

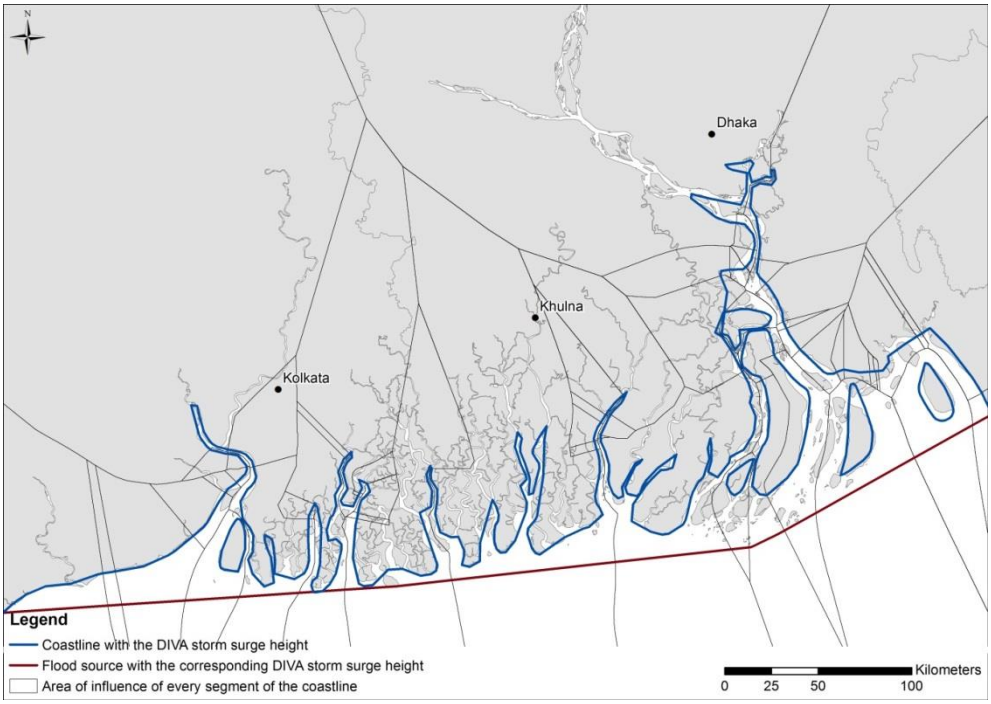

Fig S12 Representation of the DIVA coastline (blue), the flood source (red) and the areas of influence of every segment of the DIVA coastline (black lines).

3. Supplementary results for the 1 in 10 and 1 in 1000 year storm surges

Table S1: Results of the analysis for the three storm surge return periods, 1 in 10, 100 and 1000 year. The population corresponds to the number of people benefiting from flood risk mitigation by tidal wetlands. The percentage is calculated relative to the total number of people flooded in the case of the scenario 1, i.e. with the presence of the tidal wetlands. The surface corresponds to the square kilometers of land area (excluding the tidal wetlands area itself) benefitting from flood risks mitigation by the tidal wetlands. The percentage of surface area is calculated relative to the land area (excluding the tidal wetlands area itself) flooded in the case of the scenario 1.

		Population (number of people)			Population (relative %)			Surface (km²)			Surface (relative %)		
Delta	Country	1 in 10 year	1 in 100 year	1 in 1000 year	1 in 10 year	1 in 100 year	1 in 1000 year	1 in 10 year	1 in 100 year	1 in 1000 year	1 in 10 year	1 in 100 year	1 in 1000 year
Ganges-Brahmaputra	India and Bangladesh	1,114,765	1,322,735	1,541,264	16.3	16.8	15.4	1,538.7	1,820.9	1,538.7	19.0	19.5	19.0
Yangtze	China	4,438,443	5,922,009	7,322,102	49.1	49.1	49.0	7,177.2	9,126.8	11,176.1	58.8	59.4	59.0
Mekong	Vietnam	4,172,316	4,602,641	4,927,996	26.3	25.4	24.7	12,578.2	13,775.4	14,650.4	41.9	40.7	39.6
Chao Phraya	Thailand	1,079,150	1,300,156	1,644,581	74.7	76.2	74.4	1,414.9	1,665.6	2,002.2	85.3	86.2	86.0
Irrawaddy	Myanmar	223,766	274,041	293,823	9.7	9.5	8.9	1,593.2	2,022.8	2,163.0	17.4	17.3	16.3
Niger	Nigeria	913,558	927,175	951,743	89.7	89.4	89.4	924.5	942.4	981.7	99.3	99.4	99.4
Amazon	Brazil	44,289	45,286	46,663	12.3	12.2	12.5	1,832.7	2,109.4	2,373.4	17.4	17.6	18.1
Rhine	The Netherlands	339,604	383,869	418,280	6.6	6.9	7.2	986.5	1,043.6	1,093.2	12.7	12.8	12.9
Mississippi	USA	148,637	235,452	248,607	59.0	58.1	59.2	3,467.6	4,334.5	5,051.6	84.7	82.8	80.2
Mahakam	Indonesia	175,773	238,500	240,363	98.4	98.0	97.7	375.6	525.2	553.7	94.8	94.3	94.7
Burdekin	Australia	164	169	188	49.7	46.8	46.5	65.9	70.7	89.0	55.7	53.4	49.9

4. Supplementary analysis of the sensitivity of the model

In order to compare the flood-exposed areas predicted by the GIS model and the areas that can be indeed flooding during flood events, the flooding extend of two cyclones were selected, the cyclone Sidr of November 2007 for the Ganges-Brahmaputra and the cyclone Nargis of May 2008 for the Irrawaddy delta. The result of this comparison shows that about 50 % of the areas that were flooded during those cyclone events are flood-exposed areas predicted by the model (Figure 2). While the model is not designed to predict the areas that are indeed flooded during specific flood events (which largely depends on the failure of flood protecting structures like dikes and dams present in both deltas), it is able to designate as flood-exposed areas those areas that indeed experienced storm surge flooding from specific cyclone events. It should be further noticed that, in the two deltas, the areas actually flooded by the cyclone events are a combination of flooding caused by both the storm surge and the rainfall driven fluvial floods, and the latter is not accounted for in our modelling approach.

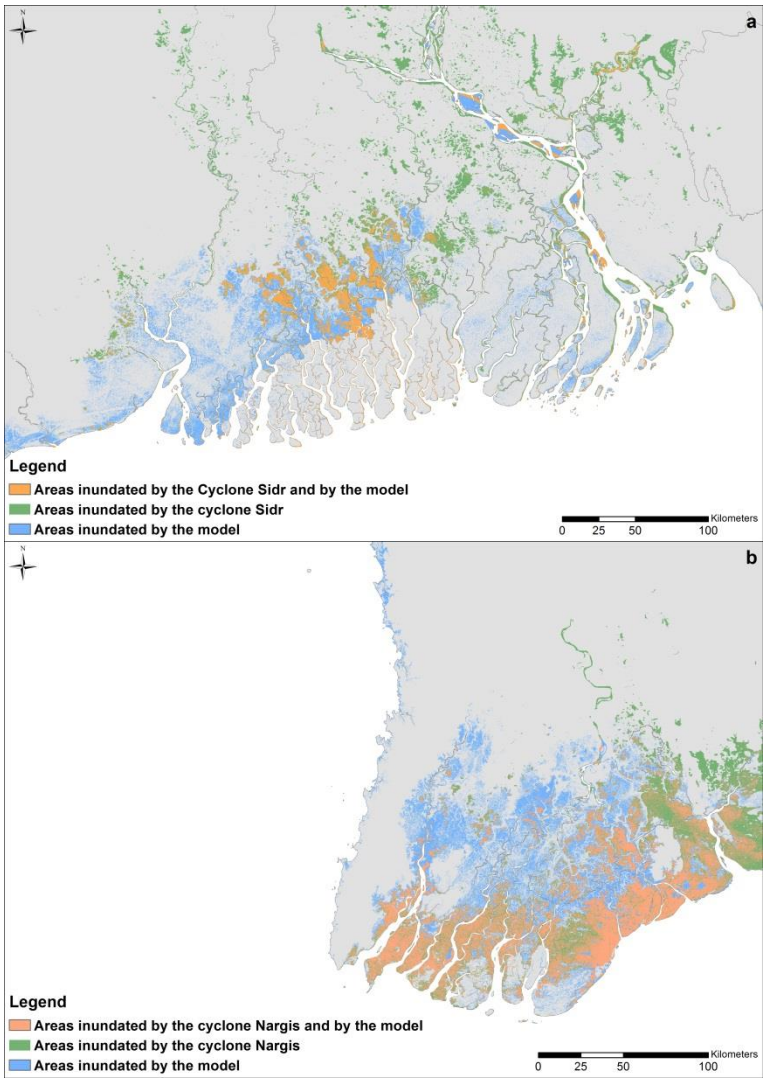

Fig S13 Comparison of the delta's flood-exposed areas predicted by the GIS model and the areas flooded during previous cyclone events for (a) the Ganges-Brahmaputra delta with the cyclone Sidr (15/11/2007) and (b) the Irrawaddy delta with the cyclone Nargis (02/05/2008).